

1 **A conceptual, distributed snow redistribution model**

2 **S. Frey¹ and H. Holzmann¹**

3 [1]{Institute of Water Management, Hydrology and Hydraulic Engineering, University of
4 Natural Resources and Life Sciences, Vienna, Austria}

5 Correspondence to: S. Frey (simon.frey@boku.ac.at)

6

7 **Abstract**

8 When applying conceptual hydrological models using a temperature index approach for
9 snowmelt to high alpine areas often accumulation of snow during several years can be
10 observed. Some of the reasons why these “snow towers” do not exist in nature are vertical and
11 lateral transport processes. While snow transport models have been developed using grid cell
12 sizes of tens to hundreds of square meters and have been applied in several catchments, no
13 model exists using coarser cell sizes of one km², which is a common resolution for meso and
14 large scale hydrologic modelling (hundreds to thousands of square kilometres). In this paper
15 we present an approach that uses only gravity and snow density as a proxy for the age of the
16 snow cover and land-use information to redistribute snow in Alpine basins. The results are
17 based on the hydrological modelling of the Austrian Inn basin in Tyrol, Austria, more
18 specifically the Ötztaler Ache catchment but the findings hold for other tributaries of the river
19 Inn. This transport model is implemented in the distributed rainfall-runoff model COSERO.
20 The results of both model concepts with and without consideration of lateral snow
21 redistribution are compared against observed discharge and snow covered areas derived from
22 MODIS satellite images. By means of the snow redistribution concept snow accumulation
23 over several years can be prevented and the snow depletion curve compared with MODIS
24 data could be improved, too. In a seven year period the standard model would lead to snow
25 accumulation of approximately 2900 mm SWE in high elevated regions whereas the updated
26 version of the model does not show accumulation and does also predict discharge with more
27 accuracy leading to a Kling-Gupta-Efficiency of 0.93 instead of 0.9. A further improvement
28 can be shown in the comparison of MODIS snow cover data and the calculated depletion
29 curve, where the redistribution model increased the efficiency (R^2) from 0,70 to 0,78
30 (calibration) and from 0,66 to 0,74 (validation).

1

2 **1 Introduction**

3 Conceptual models are widely used in hydrology. Examples are the HBV model (Bergström,
4 1976), PDM (Moore, 2007), GSM-SOCONT (Schaeffli et al., 2005) or VIC (Wood et al.,
5 1992) just to name a few. Many of these conceptual models use a temperature index approach
6 to model snow melt and snow accumulation and even in some physically based models as
7 e. g. versions of the SHE model (Bøggild et al., 1999) this method can be found. This
8 approach has the advantage of being quite simple since it uses only temperature as input to
9 determine whether precipitation occurs in the form of snow or rain and whether snow can be
10 melted or not. A typical example of a temperature index method for snow modelling is the
11 degree-day approach (see for example Hock 2003). A disadvantage is that snow accumulates
12 as long as the air temperature does not rise above a certain threshold (often 0 °C) regardless of
13 any other processes that may lead to snow melt like radiation or turbulent fluxes of latent
14 energy. In high mountainous areas this may be the case for most days in the year leading to an
15 intensive computational accumulation of snow in these areas. In the modellers terminology
16 these artefacts are often called “snow towers”. In nature, however, these accumulations are
17 barely existent.

18 The reasons for that are either wind or gravitationally induced lateral snow distribution
19 processes (Elder et al., 1991; Winstral et al., 2002). Resulting snow depths are not uniformly
20 distributed in space but vary within large ranges (Helfricht et al., 2014). When changing the
21 focus from micro (e. g. several square meters) to meso scales (e. g. one to several square
22 kilometres), variations become less (Melvold and Skaugen, 2013). The intention of the
23 applied snow redistribution concept was (i) to prevent the artefacts of “snow towers” and (ii)
24 to develop a concept which considers gravity driven lateral snow transport with reasonable
25 and plausible process depiction.

26 **1.1 Theoretical background of snow cover variations**

27 During the accumulation period, according to Liston (2004), primarily three mechanisms are
28 responsible for these variations: (i) snow-canopy interactions in forest covered regions, (ii)
29 wind induced snow redistribution and (iii) orographic influences on snow fall. These
30 mechanisms influence snow cover patterns on scales ranging from the micro to the macro
31 scale. Spatial snow cover variability beneath canopies is mainly affected by different tree

1 species (deciduous vs coniferous trees) influencing LAI, height and density of the canopy and
2 gap sizes (Garvelmann et al., 2013; Liston, 2004; Pomeroy et al., 2002).

3 Besides the impact of vegetation, wind is the most dominant factor influencing snow patterns
4 in alpine terrain. Snow is transported from exposed ridges to the lee side of these ridges,
5 valleys and vegetation covered areas (Essery et al., 1999; Liston and Sturm, 1998; Rutter et
6 al., 2009; Winstral et al., 2002). One has to be aware that besides of the physical transport of
7 solid snow wind also stimulates sublimation processes (Liston and Sturm, 1998; Strasser et
8 al., 2008). Wind influences snow depth distributions on scales of some 100s to 1000 square
9 metres (Dadic et al., 2010a).

10 The third mechanism (orographic effect) influences snow patterns on a larger scale of one to
11 several kilometres (e. g. Barros and Lettenmaier, 1994). Non-uniform snow distributions are
12 caused by interactions of the atmosphere (air pressure, humidity, atmospheric stability) with
13 topography (Liston, 2004).

14 In addition to these processes, avalanches play a role in snow redistribution (Lehning and
15 Fierz, 2008; Lehning et al., 2002; Sovilla et al., 2010). In steep terrain, avalanches depend
16 mainly on the slope angle and are capable of transporting large snow masses over distances of
17 tens to hundreds of metres (Dadic et al., 2010b; Sovilla et al., 2010).

18 During the ablation period, spatial snow distributions are mainly influenced by differences in
19 snow melt behaviour. On the northern hemisphere, on south-facing slopes, rates of snow melt
20 are generally enhanced compared to north-facing slopes due to the inclination of radiation.
21 Also vegetation influences melting behaviour. Shading reduces snowmelt compared to direct
22 sunlight. Enhanced emitted long wave radiation due to warm bare rocks or trees increases the
23 melt rate (Garvelmann et al., 2013; Pohl et al., 2014).

24 **1.2 Modelling approaches**

25 There exist a plenty of model concepts to simulate the snow redistribution in mountainous
26 areas, ranging from simple conceptual models to complex, physically based ones. The latter
27 attempt to consider all energy fluxes and therefore show a huge data demand with respect to
28 meteorological input. Usually this type requires high spatial resolution of the model domain.
29 Alternatively the conceptual models can also be easily applied for meso and macro scale
30 basins, where the spatial resolution generally shows coarser grid spacing. This is the case for

1 the introduced study where the entire basin of the river Inn was modelled (see Frey et al.,
2 2014) and selective results of the Ötztal are presented.

3 Generally, there are several ways of coping with intensive snow accumulations in
4 hydrological models, in particular (i) adapting the meteorological input data, (ii) the
5 application of physically based models to solve the full energy balance and considering the
6 wind induced snow drift and (iii) conceptual models using topographic information for lateral
7 snow transport. In the following some descriptions and references of the respective concepts
8 are given.

9 A common approach is editing the meteorological input (Dettinger et al., 2004). For instance,
10 many models use a constant yet adjustable lapse rate for interpolating temperature with
11 elevation (Holzmann et al., 2010; Koboltschnig et al., 2008). Besides temperature,
12 precipitation gradients are often adjusted to fit observed and modelled target variables (e. g.
13 snow patterns or runoff) (Huss et al., 2009b; Schöber et al., 2014). Justification for doing so is
14 the general lack of gauging stations in the summit regions (Daly et al., 1994, 2008) along with
15 the high error of precipitation gauges (Rasmussen et al., 2011; Williams et al., 1998). An
16 approach presented by Jackson (1994) defining a precipitation correction matrix was
17 successfully applied in several studies (Farinotti et al., 2010; Huss et al., 2009a). Using a
18 Doppler X-band radar capable of a spatial resolution of 75 m Scipi3n et al. (2013) identified
19 significant discrepancies between precipitation patterns in 300 to 600 metres above ground
20 and the snow accumulation at the end of the winter period in a small area of 1.5 km² in the
21 vicinity of Davos, Switzerland. They conclude that snowfall variability at the height of some
22 hundreds of meters above ground is not the driving factor of snow accumulation variabilities
23 at the scale of the radar's resolution. Consequently, the variability of the meteorological input
24 cannot explain the variability of snow cover patterns.

25 Models trying to deal with snow accumulation and redistribution apart from input corrections
26 may be classified into two major approaches. One is the consideration of process based snow
27 distribution patterns. Examples are SNOWPACK (Bartelt and Lehning, 2002) used in
28 avalanche research or SnowTran3D (Liston et al., 2007; Liston and Sturm, 1998). The other
29 approach is empirical. Models following the second approach use the fact, that snow patterns
30 resemble each other every year (Helfricht et al., 2012, 2014). Since our model is following the
31 empirical approach, too, the presented paper concentrates on that approach.

1 Snow accumulation gradients determined by airborne LiDAR measurements (Helfricht et al.
2 2012) were used by Schöber et al. (2014) to improve hydrological modelling using the
3 distributed energy balance model SES (Asztalos, 2004). LiDAR data, however, are relatively
4 expensive to obtain. A common way of dealing with snow accumulations without the need for
5 intensive field campaigns is using wind speed and -direction to model lateral snow transport
6 (e.g. Bernhardt et al., 2009; 2010; Shulski and Seeley, 2004; Winstral et al., 2002; Liston and
7 Sturm, 1998). Wind information may be obtained by meteorological stations or by computed
8 wind fields. Kirchner et al. (2014) concluded from LiDAR measurements in combination with
9 meteorological stations in a catchment in California, USA that wind measurements from only
10 one meteorological station are of too poor quality for a useful description of wind fields for
11 snow transport. Due to the mentioned lack of meteorological stations in high elevations, the
12 use of computer generated wind fields seems appealing. These information have been
13 successfully used to model snow redistributions in small scales of 30 metres (Bernhardt et al.,
14 2009, 2010, 2012). Those models using wind information have in common that they are
15 computationally intensive as they require data in high spatial resolution (e. g. 100 to 1000s of
16 square metres). Wind fields may also be generated by regional circulation models (RCM).
17 However these wind fields have shown to be erroneous (Nikulin et al., 2011) and therefore
18 are not useful for direct implementation in redistribution models. A combined approach using
19 gravity and wind induced snow transport was presented by Schöber et al. (2014) who used a
20 distributed energy balance model with a resolution of 50x50 m. The SnowSlide model
21 (Bernhardt and Schulz, 2010) applied to the Watzmann massif, Germany, even only accounts
22 for gravitational induced snow transport.

23 The mentioned model approaches have in common that they operate on spatial scales of 10s
24 to 100s of metres. However, due to some available databases for vegetation and meteorology
25 (Haiden et al., 2011; Hiebl and Frei, 2015; Masson et al., 2003; Oubeidillah et al., 2014),
26 many models operate on cell sizes of 1 km² or more (e. g. Andersen et al., 2001; Henriksen et
27 al., 2003; Mauser and Bach, 2009; Safeeq et al., 2014). While the main driving physical
28 processes on the scale of these datasets might differ from the scale of the modelling
29 approaches described above the difficulties of snow accumulations also occur when models
30 with grid cell sizes of 1x1 km are applied to mountainous regions. Yet, to our knowledge, no
31 model for redistributing snow on a 1x1 km grid size exists. In this paper we present a simple
32 approach to deal with snow in high mountainous regions and its application in the catchment
33 of Ötztaler Ache in Tyrol, Austria. Since the model uses meteorological input from INCA

1 (Haiden et al., 2011) that already account for meteorological corrections, we focus on snow
2 redistribution rather than to edit the input data. As already mentioned the two main objectives
3 in this respect are to achieve a better model efficiency regarding runoff and to avoid the
4 existence of snow towers at high altitudes.

5

6 **2 Model description**

7 **2.1 Hydrological Model COSERO**

8 COSERO is a spatially distributed conceptual hydrological model which is similar to the
9 HBV model (Bergström, 1976). In the presented paper it uses 1x1 km grid cells. Originally
10 developed for modelling discharge of the Austrian rivers Enns and Steyer (Nachtnebel et al.,
11 1993), it has recently been used for different purposes like climate change studies (e. g. Kling
12 et al., 2012, 2014b; Stanzel and Nachtnebel, 2010), investigating the role of
13 evapotranspiration in high alpine regions (Herrnegger et al., 2012) and operational runoff
14 forecasting (Stanzel et al., 2008). Potential evapotranspiration is calculated using the
15 Thornthwaite method (Thornthwaite, 1948). Discharge due to rainfall and snow-/ice melt is
16 estimated using the same non-linear function of soil moisture as the original HBV. In this
17 study, the model is run using daily time steps. It is, however, capable of using hourly or
18 monthly time steps. In the latter case, intra-monthly variations are considered for snow and
19 interception processes as well as for soil moisture (Kling et al., 2014a). A schematic overview
20 of the model is given by Fig. 1 and a detailed description of the model can be found in Kling
21 et al. (2014a), where the model was applied to several catchments across Europe, Africa and
22 Australia. However, in Kling et al. (2014a) snow parameters were not calibrated and therefore
23 the snow module is not fully explained in detail in their paper. This will be done in the
24 following. Equations (1) to (7) and (10) were taken from the original model by Stanzel and
25 Nachtnebel (2010), all other methods were developed in the present study.

26 Numerous studies have shown that sub-grid variability of snow depths can be described by a
27 two parameter log-normal distribution (e. g. Donald et al., 1995; Pomeroy et al., 1998).
28 COSERO uses five snow classes per cell (i.e. the log-normal distribution is subdivided into
29 five quantiles) to approximate this sub-grid log-normal distribution under accumulation
30 conditions (see Fig. 2 b)), i. e. snowfall is distributed log-normally into snow classes, where
31 the sum of the snow water equivalent (SWE) of each classes represent the mean conditions in

1 the grid cell. This distribution can be interpreted as a statistical description of snow
 2 distribution processes taking place at the subgrid scale (Pomeroy et al., 1998). This method
 3 has the potential to indirectly consider the influence of curvature, shelter, vegetation or
 4 elevation (Hiemstra et al., 2006). The properties of each class are treated unique as equations
 5 (1) to (13) apply to every snow class separately. Consequently the log-normal distribution
 6 within a grid cell may be disturbed by the processes of melting, sublimation, refreezing and
 7 redistribution to other grid cells. Once fallen, snow redistribution between the snow classes
 8 within a single grid cell is not considered. A scheme of the composition of a snow class is
 9 illustrated in Fig. 2 a). The snow water equivalent (S_{SWEt}) of a given day t per class is
 10 calculated by Eq. (1) where P_{Rt} and P_{St} are liquid and solid precipitation in mm, respectively,
 11 M_t is snow melt and E_{St} is sublimation of snow. All variables are given in mm SWE.

$$12 \quad S_{SWEt} = S_{SWE_{t-1}} + P_{Rt} + P_{St} - M_t - E_{St} \quad (1)$$

13 Snow melt is calculated by a temperature index approach (see for example Hock 2003). Eq.
 14 (2) is used:

$$15 \quad M_t = \min(S_{SWEt}; P_{Rt} \cdot \varepsilon \cdot T_{AIRt} + D_{ft} \cdot T_{AIRt}) \quad (2)$$

16 where M_t is snowmelt [mm], ε is the ratio of specific heat of water and melting energy, T_{AIRt}
 17 is the (mean) daily air temperature [$^{\circ}\text{C}$] and D_{ft} [$\text{mm } ^{\circ}\text{C}^{-1}$] is the snow melt factor of a given
 18 day t estimated by Eq. (3):

$$19 \quad D_{ft} = \left(-\cos\left(J \cdot \frac{2\pi}{365}\right) \cdot \frac{D_U - D_L}{2} + \frac{D_U - D_L}{2} \right) \cdot M_{REDt} \quad (3)$$

20 with

$$21 \quad M_{REDt} = \begin{cases} D_{RED}, & S_{fresh} \geq S_{CRIT} \\ M_{RED_{t-1}} + \frac{(1 - M_{RED_{t-1}})}{5}, & S_{fresh} < S_{CRIT} \end{cases} \quad (4)$$

22 where J is the Julian day of the year [-], D_U and D_L are the upper and lower boundaries of D_f
 23 [$\text{mm } ^{\circ}\text{C}^{-1}$], respectively, and M_{RED} [-] is a reduction factor to account for the higher albedo
 24 caused by freshly fallen snow calculated by Eq. (4). S_{CRIT} [mm] is the critical snow depth of
 25 fresh snow necessary to increase the albedo, whereas S_{fresh} is the actual depth of fresh snow
 26 [mm] fallen within one time step. For fresh snow depth larger than S_{CRIT} , M_{RED} is set to a
 27 reduced melting factor D_{RED} [-].

1 Whether precipitation occurs in form of snow or rain is controlled by two parameters T_{PS} and
 2 T_{PR} , defining the temperature range where snow and rain occur simultaneously. At and above
 3 temperature T_{RP} precipitation is pure liquid, at and below T_{PS} precipitation is pure solid. In
 4 between those two boundaries, the proportion of solid to liquid precipitation is estimated
 5 linearly.

6 For the estimation of snow sublimation, Eq. (5) is used, where E_{SP} [mm] refers to potential
 7 sublimation of snow, E_P [mm] is the potential evapotranspiration and E_R is a correction factor
 8 to reduce E_P . Sublimation is considered only for snow classes actually covered by snow.
 9 Hence, if a grid cell is partly snow free (this can be the case if one subgrid class has no snow
 10 cover due to melting) sublimation is estimated for the snow covered part only. For the
 11 uncovered classes evapotranspiration according to the Thornthwaite method is applied.

$$12 \quad E_{SP_t} = E_{P_t} \cdot E_R \quad (5)$$

13 The snow cover in COSERO is treated as porous medium and therefore is able to store a
 14 certain amount of liquid water (S_l [$m^3 \text{ kg}^{-1}$]) in dependency of the snow pack density (ρ)
 15 calculated using Eq. (6).

$$16 \quad S_{l_t} = (S_{SWE_t} - S_{l_{t-1}}) \cdot (S_{lMAX} - (\rho - \rho_{MAX}) \cdot S_{l\rho}) \quad (6)$$

17 Where S_{lMAX} [$m^3 \text{ kg}^{-1}$] is the maximum water holding capacity at the maximum snow density
 18 of the snow pack ρ_{MAX} [kg m^{-3}] and $S_{l\rho}$ [-] describes the decrease of water holding capacity
 19 with increasing snow density ρ .

20 At negative air temperatures, retained melt water has the ability to refreeze in the snow pack.
 21 The potential amount of refrozen water (S_R) is estimated by Eq. (7), where R_f is the refreezing
 22 factor [$\text{mm } ^\circ\text{C}^{-1}$]. As long as there is enough liquid water in the snow pack, actual refreezing
 23 will be equal to potential refreezing.

$$24 \quad S_R = \begin{cases} 0, & T_{AIR_t} > 0 \\ R_f \cdot (T_{AIR_t} \cdot (-1)), & T_{AIR_t} \leq 0 \end{cases} \quad (7)$$

25 Refrozen water is treated in the same way as snow. The amount of water leaving the snow
 26 cover then equals snowmelt minus retained water.

27 Snow density (ρ_t) of each class is calculated using a sigmoid function shown in Eqs. (8) and
 28 (9) where ρ_{MAX} and ρ_{MIN} are the respective maximum and minimum values of ρ , T_{AIR} is the
 29 temperature of the air mass above the snow layer and ρ_{scale} and T_{scale} are scaling coefficients

1 to calculate a transition temperature (T_{tr}) for the estimation of the snow density. Herby, ρ_{scale}
 2 adjusts the slope of the function, whereas T_{scale} is responsible for a shift on the x-axis. These
 3 two parameters are set to fixed values of 1.2 and 1, respectively. The solution of Eqs. (8)
 4 and (9) is illustrated in Fig. 3 for a range of typical air temperatures, where snowfall occurs.
 5 Already fallen snow can reach a higher density (ρ_{OLD}) than fresh snow. Its density is
 6 calculated using a time settling constant (ρ_{SET} , derived from Riley et al., 1973) until the
 7 maximum density is reached (Eq. 10).

$$8 \quad \rho_t = (\rho_{MAX} - \rho_{MIN}) \cdot \left(\frac{T_{tr}}{\sqrt{1+(T_{tr})^2}} + 1 \right) \cdot 0.5 + \rho_{MIN} \quad (8)$$

9 with

$$10 \quad T_{tr} = \frac{T_{AIR_t}}{\rho_{scale}} + T_{scale} \quad (9)$$

$$11 \quad \rho_{OLD} = \frac{\rho_{SET} \cdot \left(\frac{SWE_t + S_t}{\rho_{OLD} + 2} \right)}{1 + \frac{\rho_{SET}}{2}} \quad (10)$$

12 The COSERO model considers both snow and glacier ice melt processes. Ice melt (M_{ICE}) is
 13 computed by means of a degree-day method (see Eq. 11) and uses separate parameter sets.
 14 Here, D_{ICE} refers to the ice melt factor [$\text{mm } ^\circ\text{C}^{-1}$]. A prerequisite of ice melt is the full
 15 depletion of the overlying snow cover. Spatial information of glaciers are taken from the
 16 Randolph Glacier Inventory version 3.2 (Arendt et al., 2012).

$$17 \quad M_{ICE} = D_{ICE} \cdot T_{AIR} \quad (11)$$

18 **2.2 Snow transport model**

19 Several authors reported that the slope angle has an important influence on snow depths
 20 (Bernhardt and Schulz, 2010; Kirchner et al., 2014; Schöber et al., 2014). The model
 21 redistributes snow only to grid cells providing the steepest slope (acceptor cell) in the direct
 22 neighbourhood of the raster cell it searches from (donor cell). Only downward transportation
 23 is considered. If more than one cell show the same (largest) difference in elevation, the
 24 amount of donated snow is distributed equally to the number of acceptor cells. The actual
 25 amount of snow being redistributed depends on the steepness of the slope, the age of the snow
 26 cover, considered by the density of snow, the type of land cover of the donor cell and the
 27 snow depth of the donor cell. The drier (less dense) the snow pack the higher the snow rate
 28 available for the redistribution routine (f_p , Eq. 13). Thus the defined maximum density of

1 snow (450 kg m^{-3}) determines the threshold for snow redistribution. The availability of snow
 2 for transport is determined by a vegetation-based threshold value (H_v) for each class of land
 3 cover. This value can also be interpreted as a roughness coefficient for areas where no or
 4 hardly any vegetation is present like in alpine and nival elevations. If the snow depth (S
 5 [mm]) of a snow class of a raster cell exceeds H_v [mm], snow transport from that cell is
 6 activated and redistribution is calculated by solving Eqs. (12) and (13).

$$7 \quad = \max(S_D - H_v; 0) \cdot f_\rho \cdot \frac{1}{\Sigma A} \cdot C \quad (12)$$

8 With

$$9 \quad f_\rho = \left(\frac{(\rho_{MAX} - \rho_D)}{\rho_{MAX}} \cdot e^{\left(-\frac{\rho_D}{\rho_{MAX}} \right)} \right) \cdot \frac{\alpha}{90} \quad (13)$$

10 Where $S_{SWE(A)}$ is the amount of snow water equivalent that is redistributed from the donor cell
 11 (D) to the available acceptor cell(s) (A), ρ_D is the density of snow in the donor cell, ρ_{MAX} is
 12 the possible maximum density of snow, α is the angle of the slope between the donor and
 13 acceptor cells in degree and C is a correction coefficient that can be calibrated.

14 Fig. 4 illustrates the shape of the distribution coefficient f_ρ as a function of different elevation
 15 gradients between the acceptor and donor cells and of the snow density. In acceptor cells
 16 redistributed snow is treated as fresh snow in the sense that it is distributed to the snow
 17 classes according to the log-normal distribution.

18 The model is organized in form of a loop starting at the highest grid cell (summit region) and
 19 ending at the lowest cell (outlet of the catchment). This ensures that snow cannot be
 20 redistributed into already processed grid cells. Snow will be transported downslope as long as
 21 the slope is steep enough to allow for transportation given that the density of snow is low
 22 enough (see Fig. 4). Consequently less snow remains in the summit region whereas lower,
 23 rather flat grid cells show enhanced accumulation. Although snow depths in the summits are
 24 lower, the amount of snow covered cells stay similar as some residual snow remains in all
 25 cells due to H_v parameterization.

26 The concept of the redistribution model is sketched in Fig. 5. Note that although snow depths
 27 in the highest cell are prevented by the model, the number of snow covered cells remains the
 28 same.

29

1 **3 Case study in the catchment the Ötztaler Ache, Tyrol, Austria**

2 **3.1 Catchment description**

3 The catchment of Ötztaler Ache at gauge Huben, situated in western Austria close to the
4 Italian border, covers an area of 511 km² and has an altitudinal range between 1185 m a.s.l at
5 the gauge at Huben and 3770 m a.s.l at its highest peaks. Due to the use of a 1x1 km gridded
6 DEM, the highest grid cell has a mean elevation of 3450 m a.s.l, whereas the lowest cell has
7 an elevation of 1250 m a.s.l. (Fig. 6). About 30 % of its area is covered by vegetation, mainly
8 pastures and meadows. Glaciers cover about 19 % leading to an annual ice melt contribution
9 of about 25 % of the total runoff at Huben, while 41 % of the discharge has its origin in
10 snowmelt (Weber et al., 2010). Table 1 gives an overview of the land cover.

11 In Fig. 6 the elevations of the Ötztal basin are described. Frequency distribution of slope
12 angles derived from 1x1 km grid are shown (6 a). This frequency distribution exhibits the
13 highest frequencies in the slope classes between 20 and 25 degrees for higher elevations. In
14 lower elevated regions slope classes between 0 and 15 degrees dominate. However, also
15 glacier covered areas at the summits can have flat slopes. Note that the listed slopes are based
16 on the steepest vertical gradients of the neighbour elements.

17 **3.2 Input data**

18 Gridded meteorological data of precipitation and air temperature are required to run the
19 model. These data are provided by the INCA dataset (Haiden et al., 2011) with the same grid
20 spacing like the hydrological model, allowing a direct use in the model without the need for
21 pre-processing. INCA data are available since 2003. The years 2003 and 2004 have been used
22 as a warm-up period for the model. In the subsequent years no correction of meteorological
23 data was done since INCA already accounts for elevation gradients regarding air temperature
24 and precipitation. Six land use classes were derived from the most recent CORINE data set
25 (CLC2006 version 17, see EEA, 1995). These classes and their areal fractions in the
26 catchment of Ötztaler Ache are given in Table 1. It should be pointed out, that neither
27 radiation nor wind speed or wind direction data are necessary to run the model.

1 **3.3 Model calibration**

2 The hydrological model was calibrated for the period from 2005 to 2008 using a
3 Rosenbrock's automated optimization routine (Rosenbrock, 1960). Although the model is rich
4 of parameters, the vast majority of them have been estimated *a priori* according to literature
5 (Liston and Sturm, 1998; Prasad et al., 2001) and previous work on the model (Fuchs, 2005;
6 Kling, 2006; Nachtnebel et al., 2009). In the snow model including snow redistribution only
7 six parameters have been calibrated: upper and lower boundaries of snow melt factors D_U and
8 D_L , respectively, the threshold values that control the range where liquid and solid
9 precipitation occur simultaneously (T_{PR} , T_{PS}), the standard deviation of the log-normal
10 distribution of snow depth in one grid cell (N_{VAR}) and the calibration parameter for snow
11 redistribution C (see Eq. 12). The limited number of optimization parameters reduces
12 equifinality problems. For a more detailed description of equifinality issues see the
13 supplements of this article. The target of the calibration was a good fit of runoff using the
14 Kling-Gupta-Model-Efficiency (Gupta et al., 2009; Kling et al., 2012) as objective function.
15 The model was validated for the years 2009 and 2010. Both calibration and validation have
16 been done with and without using the snow transport module. In the following model A refers
17 to the model using snow transport, whereas model B stands for the standard model.
18 Vegetation threshold values for snow detention were taken from previous studies (Liston and
19 Sturm, 1998; Prasad et al., 2001). These are given in Table 1. Maximum snow density was
20 assumed 450 kg m^{-3} which matches long term snow measurements (Jonas et al., 2009;
21 Schöber et al., 2014). Besides discharge in the validation period also snow cover data from
22 MODIS (8 day maximum snow cover, version 5) satellite images (Hall et al., 2002) were used
23 to compare the performance of both models.

24

25 **4 Results**

26 **4.1 Discharge**

27 Fig. 7 shows a comparison of total discharge using model A and B at the gauge Huben for the
28 year 2006. Both models result in similar quality criteria in the calibration as well as in the
29 validation period (see Table 2). Nevertheless, the model efficiency could be improved by 0.05
30 in the calibration period and 0.02 in the validation period by accounting for lateral snow
31 transport. Maximum differences in the mean daily discharges between the two models reach

1 up to 2 mm per day ($12.1 \text{ m}^3 \text{ s}^{-1}$). This equals a relative difference of -9 up to 44 % of model
2 A in respect to model B. In total, model A generates a surplus of about 300 mm discharge in
3 five years compared to model B (Fig. 8). About 2/3 of the additional discharge originate in
4 enhanced snowmelt the rest occurs due to enhanced glacier melt.

5 **4.2 Spatially distributed snow cover data**

6 Fig. 9 compares model A and B with MODIS snow depletion data. Both the accumulation
7 period in winter and the ablation period in spring and summer are represented well by both
8 models. Cold snowfall periods in summer generate sharp peaks in the depletion curve, which
9 could be calculated by both model versions, where Model A computed slightly smaller peaks
10 during the snowmelt period (May to July). This leads to a moderate increase of the
11 determination factor R^2 from 0.70 to 0.78 (calibration) and from 0.66 to 0.74 (validation).

12 **4.3 Inter annual snow accumulation**

13 The main reason for developing a snow transport model was the prevention of “snow towers”.
14 Fig. 10 presents model behaviour of model A and B with respect to the accumulation of snow
15 in elevations above 2800 m a.s.l. Below that elevation none of the models indicates snow
16 accumulation for more than one year and therefore snow accumulation in lower altitudes is no
17 problem. By the end of seven years of modelling, model B shows snow depths of approx.
18 2900 mm SWE in elevations above 3400 m a.s.l. whereas model A does hardly show any
19 accumulation behaviour in these altitudes. Spatially distributed net loss and gain of snow for
20 all raster cells within the period of one year in the watershed are presented in Fig. 11. It can
21 be shown that net loss is evident in the zones of ridges and high elevations, where the
22 maximum net gain is along the valley bottoms.

23 **4.4 Parameter equifinality**

24 Since the model uses several parameters that need calibration it suffers from equifinality
25 issues. To investigate those issues, Monte Carlo simulations have been carried out varying the
26 snow relevant parameters that cannot be estimated a priori. Since the aim of this paper is
27 snow transport, the results of the Monte Carlo simulations can be found in the supplements of
28 this article.

29

1 **5 Discussion**

2 **5.1 Discharge**

3 In spring, at the beginning of the melting season, higher runoff is generated by the model
4 accounting for lateral snow transport (model A) due to a larger amount of snow in lower
5 altitudes (see Fig. 7). Later in the year enhanced glacier melt is mainly responsible for higher
6 discharge rates. About 200 mm have their origin in enhanced snowmelt, while the remaining
7 100 mm originate in amplified melt of glaciers. Since glacier cover about 19.4 % of the
8 catchment's area 100 mm of additional mean basin runoff corresponds to an enhanced
9 negative glacier mass balance of -500 mm. The reason for this is transport of snow in warmer
10 altitudes and therefore earlier and more snow free glacier surfaces producing higher discharge
11 due to glacier melt (see Fig. 8) and explains the peak in July and August in runoff difference
12 (see Fig 7).

13 One has to be aware that the glacier model is very simple, since it treats glaciers as surfaces
14 with infinite depths and static properties. However, besides an advanced algorithm that
15 increases model complexity, a dynamic glacier model would require high spatial resolution
16 information of both the glaciers surfaces as well as the terrain (Farinotti et al., 2009). Since
17 the intention of this paper was to develop a model operating at the 1x1 km scale, this is not
18 feasible.

19 **5.2 Spatially distributed snow cover data**

20 Fig. 9 shows the snow depletion curve of the year 2009 based on MODIS data and the
21 comparison of model runs A and B. Only little differences between model A and B can be
22 identified. The reason for this is the vegetation threshold. Even if snow is being transported, a
23 residual of snow remains in the donor cell resulting in the cell marked as snow covered. Grid
24 cells covering the summits only donate snow to their respective acceptor cells. However, a
25 certain amount of snow is held back according to the threshold due to vegetation and
26 roughness of the surface. As indicated in Fig. 5 grid cells nested in the intermediate slope
27 regions receive and donate snow at the same time. Thus their snow depth changes little if
28 comparing model A and model B. In flat valley regions, grid cells only receive snow, where
29 relatively high air temperature values often allow for melting.

1 Satellite based snow cover information by MODIS are binary and so is the model output for
2 comparing these results. In a binary system, no difference can be distinguished between cells
3 covered by much or little snow.

4 **5.3 Snow accumulation**

5 While using model B, the higher the elevation the more snow is accumulated. Contrary,
6 model A shows less pronounced and in some high altitudes even contrary behaviour (see Fig.
7 10). This is a result of the slope dependency of the distribution model. The amount of snow
8 distributed to other grid cells is higher with increasing vertical distance to the downward grid
9 cell (steeper slope). In general and in the Ötztal as well mountains are steeper in the summit
10 regions than at the bottom (see Fig. 6). Consequently in the summit regions snow will be
11 preferentially eroded while it accumulates at the rather flat valleys where the vertical
12 distances between the grid cells are less than at the peaks. This does reflect snow
13 accumulations that can be observed in nature where summits might be nearly snow free in
14 spring while flatter parts are still covered with snow. While the raster cells covering peak
15 regions act as donators only those cells located on slopes may receive and distribute snow at
16 the same time (Fig. 11). Valley regions only receive snow. The resulting net loss and gain
17 areas shown in Fig. 11 give some indication that the redistribution algorithm is plausible.

18 Although snow accumulation behaviour of model A is more realistic than model B snow
19 accumulation can still be observed in the highest elevations zone (see Fig. 10). This is based
20 on the parameterization of the snow holding capacity H_v , where even bare ground assigns a
21 value of 200 mm (see Table 1). The influence of the highest elevation class (> 3400 m a.s.l.)
22 on both the hydrograph and snow covered area however is very small, since this elevation
23 level is represented by only 0.78 % of the catchment's area. Consequently the objective
24 function during calibration using an automated optimization routine like Rosenbrock's routine
25 does not differ much when underestimating the correction coefficient in these grid cells.

26 The smaller the portion of high altitude areas in a catchment compared to the total catchment
27 area the less important is snow redistribution for modelling runoff. The catchment of river
28 Inn, for instance, covers an area of about 10000 km² yet only 733 km² are located at
29 elevations where intensive snow accumulations and mobilizations occur (above
30 2800 m a.s.l.). In the Ötztal basin 204 out of 511 km² are located higher than 2800 m a.s.l. If
31 model B is applied to the catchment of river Inn in five years of modelling about 15 mm SWE

1 (with respect to the entire river basin) remain in the catchment due to snow accumulation
2 processes instead of 300 mm in the Ötztal. These findings are based on an applied research
3 project for the Austrian Verbund AG, where a hydrological model was applied for the
4 assessment of the hydropower potential of the river Inn (see Frey and Holzmann, 2014; Frey
5 et al., 2014)

6 **5.4 Transferability to other catchments**

7 The model provides results that have been found by other models and field observations, too.
8 The largest snow accumulations occur at the elevation range between 2800 and 3000 m a.s.l.
9 (Fig. 10). This was also found by LiDAR measurements carried out in the same catchment
10 (Helfricht et al., 2012) as well as in several catchments in Switzerland (Grünwald et al.,
11 2014). By applying a simple hydrological model that uses elevation bands instead of raster
12 cells to a variety of other catchments in the Alps, Frey (2015) could identify this elevation
13 range, too. Given that and the needs of the model (slope angles, snow density) for transporting
14 snow, it produces valid results as long as a catchment features relatively steep slopes in the
15 summit regions (which is the case in most catchments in the Alps). Obviously, the model
16 needs calibration if it is transferred to another catchment.

17 **5.4 Parameter equifinality**

18 Like most hydrological models COSERO requires calibration of some parameters. This
19 necessarily causes equifinality issues (Beven and Freer, 2001). The more adjustable
20 parameters a model provides, the more important this problem may become (e. g. Gupta et al.,
21 2008). On the other hand, some authors pointed out that more complex models may produce
22 more feasible results if the parameters can be estimated within realistic boundaries (Gharari et
23 al., 2012, 2014; Hrachowitz et al., 2014). Applying COSERO with the presented snow
24 redistribution routine requires two additional parameters: the vegetation threshold H_V
25 (estimated *a priori*) and the calibration parameter C (see Eq. 12). Yet, accounting for snow
26 redistribution allows the modeller to use D_U values within or close to the range proposed by
27 Kling et al., (2006), while the standard version of the model leads to the best results if higher
28 and therefore unrealistic D_U values are used (see supplements of this article).

1 **5.5 Scaling issues**

2 Notwithstanding, that other geomorphological properties than slope angle influencing snow
3 patterns are important on scales smaller than the grid size of COSERO (see section 1.1), slope
4 was selected as driving force for the model. One has to be aware that this is a simplification
5 and under realistic conditions snow might not necessarily be transported only on the steepest
6 route (Bernhardt and Schulz, 2010; Winstral et al., 2002). Also the response of glaciers might
7 change when finer spatial resolutions are applied. In a study at the Blaueisferner, Germany,
8 Bernhardt et al. (2010) found additional snow getting blown on glacier surfaces when they
9 used a 30 m resolution. At the coarser resolution of 300 m this result could not be found,
10 though. However, as indicated in the introduction, the 1x1 km scale is often used when
11 hydrological models are applied to medium or large catchments of 100s or 1000s of square
12 kilometres. Not only because of a variety of existing input data sets on that resolution but also
13 for performance issues. The results of this study show that the model operating on that scale is
14 able to reproduce the spatial snow distribution patterns in the catchment and prevent the
15 model from accumulating snow over several years.

16 **6 Conclusions**

17 A model for redistribution of snow on a coarse 1x1 km raster has been developed and tested
18 in the catchment of Ötztaler Ache, Austria. While only little improvement of snow cover
19 compared to MODIS data could be achieved, appearance of “snow towers” in high altitudes
20 could be prevented. In terms of discharge at the outlet of the basin, both models show good
21 results. However, the Kling-Gupta-efficiency of model A could be improved by 0.05 in the
22 calibration and by 0.02 in the validation period. With respect to the entire watershed area the
23 model using snow redistribution generates a surplus of about 200 mm runoff originated from
24 snowmelt in five years than without considering this process. This does not only affect the
25 water balance of the catchment. Due to longer time periods where the overlaying snow cover
26 on glacier surfaces is fully depleted, glacier melt is amplified by about 100 mm in five years.
27 With respect to the glaciated area this means that glaciers lose an additional 500 mm of their
28 ice during that period. Since glaciers are represented in a very simple way in this model, these
29 results need to be treated with caution. Nevertheless, glaciers play an important role in the
30 water balance of Alpine catchments and respond on snow redistribution also on the 1x1 km
31 scale.

1 The integration of a snow transport module promotes the demand, that models work “right for
2 the right reasons” and is an attempt to integrate more real process understanding into the
3 model approach. Further work needs to be carried out with respect to validation of spatially
4 distributed snow patterns. For this purpose, satellite images from Landsat might be of use
5 providing a higher spatial resolution than MODIS.

6 Even though the vast majority of parameters were estimated *a priori* in this work, equifinality
7 remains an issue. However, redistribution of snow requires only two additional parameters but
8 allows for more realistic boundaries (see Kling et al., 2006) of the snow melt factors (see
9 supplements of this article). However, more work needs to be carried out to account for that
10 issue.

11 **Acknowledgements**

12 The authors thank their colleagues for continuing support and discussion around the coffee
13 breaks, especially to Matthias Bernhardt for friendly reviewing and commenting on the
14 manuscript. Special thanks to Herbert Formayer and David Leidinger of the institute of
15 meteorology, BOKU, for supplying the INCA data. Many thanks to Daphné Freudiger and
16 two further anonymous referees for their comments and valuable suggestions. This study was
17 part of a research project in cooperation with Verbund AG.

18

19 **References**

20 Andersen, J., Refsgaard, J. C. and Jensen, K. H.: Distributed hydrological modelling of the
21 Senegal River Basin — model construction and validation, *J. Hydrol.*, 247(3-4), 200–214,
22 doi:10.1016/S0022-1694(01)00384-5, 2001.

23 Arendt, A., Bolch, T., Cogley, J. G., Gardner, A., Hagen, J.-O., Hock, R., Kaser, G., Pfeffer,
24 W. T., Moholdt, G., Paul, F., Radić, V., Andreassen, L., Bajracharya, S., Barrand, N., Beedle,
25 M., Berthier, E., Bhambri, R., Bliss, A., Brown, I., Burgess, D., Burgess, E., Cawkwell, F.,
26 Chinn, T., Copland, L., Davies, B., De Angelis, H., Dolgova, E., Filbert, K., Forester, R. R.,
27 Fountain, A., Frey, H., Giffen, B., Glasser, N., Gurney, S., Hagg, W., D., H., Haritashya, U.
28 K., Hartmann, G., Helm, C., Herreid, S., Howat, I., Kapusti, G. G., Khromova, T., Kienholz,
29 C., Köönig, M., Kohler, J., Kriegel, D., Kutuzov, S., Lavrentiev, I., Le Bris, R., Lund, J.,
30 Manley, W., Mayer, C., Miles, E., Li, X., Menounos, B., Mercer, A., Mölg, N., Mool, P.,
31 Nosenko, G., Negrete, A., Nuth, C., Pettersson, R., Racoviteanu, A., Ranzi, R., Rastner, P.,
32 Rau, F., Raup, B., Rich, J., Rott, H., Schneider, C., Seliverstov, Y., Sharp, M., Siguossou, O.,
33 Stokes, C., Wheate, R., Winsvold, S., Wolken, G., Wyatt, F. and Zheltyhina, N.: Randolph
34 Glacier Inventory - A Dataset of Global Outliners: Version 3.2, Boulder Colorado, USA.,

- 1 2012.
- 2 Asztalos, J.: Ein Schnee- und Eisschmelzmodell für vergletscherte Einzugsgebiete, Vienna
3 University of Technology, Vienna, Austria., 2004.
- 4 Barros, A. P. and Lettenmaier, D. P.: Dynamic modeling of orographically induced
5 precipitation, *Rev. Geophys.*, 32(3), 265, doi:10.1029/94RG00625, 1994.
- 6 Bartelt, P. and Lehning, M.: A physical SNOATACK model for the Swiss avalanche warning
7 Part I: numerical model, *Cold Reg. Sci. Technol.*, 35(3), 123–145, doi:10.1016/S0165-
8 232X(02)00074-5, 2002.
- 9 Bergström, S.: Development and application of a conceptual runoff model for Scandinavian
10 catchments, SMHI Reports RHO, No. 7, Norrköping, 1976.
- 11 Bernhardt, M., Liston, G. E., Strasser, U., Zängl, G. and Schulz, K.: High resolution
12 modelling of snow transport in complex terrain using downscaled MM5 wind fields,
13 *Cryosph.*, 4(1), 99–113, doi:10.5194/tc-4-99-2010, 2010.
- 14 Bernhardt, M. and Schulz, K.: SnowSlide: A simple routine for calculating gravitational snow
15 transport, *Geophys. Res. Lett.*, 37(11), L11502, doi:10.1029/2010GL043086, 2010.
- 16 Bernhardt, M., Schulz, K., Liston, G. E. and Zängl, G.: The influence of lateral snow
17 redistribution processes on snow melt and sublimation in alpine regions, *J. Hydrol.*, 424-425,
18 196–206, doi:10.1016/j.jhydrol.2012.01.001, 2012.
- 19 Bernhardt, M., Zängl, G., Liston, G. E., Strasser, U. and Mauser, W.: Using wind fields from
20 a high-resolution atmospheric model for simulating snow dynamics in mountainous terrain,
21 *Hydrol. Process.*, 23(7), 1064–1075, doi:10.1002/hyp.7208, 2009.
- 22 Beven, K. and Freer, J.: Equifinality, data assimilation, and uncertainty estimation in
23 mechanistic modelling of complex environmental systems using the GLUE methodology, *J.*
24 *Hydrol.*, 249, 11–29, doi:10.1016/S0022-1694(01)00421-8, 2001.
- 25 Bøggild, C. E., Knudby, C. J., Knudsen, M. B. and Starzer, W.: Snowmelt and runoff
26 modelling of an Arctic hydrological basin in west Greenland, *Hydrol. Process.*, 13(12-13),
27 1989–2002, doi:10.1002/(SICI)1099-1085(199909)13:12/13<1989::AID-HYP848>3.0.CO;2-
28 Y, 1999.
- 29 Dadic, R., Mott, R., Lehning, M. and Burlando, P.: Parameterization for wind-induced
30 preferential deposition of snow, *Hydrol. Process.*, 24(June), 1994–2006,
31 doi:10.1002/hyp.7776, 2010a.
- 32 Dadic, R., Mott, R., Lehning, M. and Burlando, P.: Wind influence on snow depth distribution
33 and accumulation over glaciers, *J. Geophys. Res. Earth Surf.*, 115(1), F01012,
34 doi:10.1029/2009JF001261, 2010b.
- 35 Daly, C., Halbleib, M., Smith, J. I., Gibson, W. P., Doggett, M. K., Taylor, G. H., Curtis, J.
36 and Pasteris, P. P.: Physiographically sensitive mapping of climatological temperature and

- 1 precipitation across the conterminous United States, *Int. J. Climatol.*, 28, 2031–2064,
2 doi:10.1002/joc.1688, 2008.
- 3 Daly, C., Neilson, R. P. and Phillips, D. L.: A Statistical-Topographic Model for Mapping
4 Climatological Precipitation over Mountainous Terrain, *J. Appl. Meteorol.*, 33, 140–158,
5 doi:10.1175/1520-0450(1994)033<0140:ASTMFM>2.0.CO;2, 1994.
- 6 Dettinger, M., Redmond, K. and Cayan, D.: Winter Orographic Precipitation Ratios in the
7 Sierra Nevada—Large-Scale Atmospheric Circulations and Hydrologic Consequences, *J.*
8 *Hydrometeorol.*, 5(1992), 1102–1116, doi:10.1175/JHM-390.1, 2004.
- 9 Donald, J. R., Soulis, E. D., Kouwen, N. and Pietroniro, A.: A Land Cover-Based Snow
10 Cover Representation for Distributed Hydrologic Models, *Water Resour. Res.*, 31(4), 995–
11 1009, doi:10.1029/94WR02973, 1995.
- 12 EEA: CORINE Land Cover Project, [online] Available from:
13 <http://www.eea.europa.eu/publications/COR0-landcover>, 1995.
- 14 Elder, K., Dozier, J. and Michaelsen, J.: Snow accumulation and distribution in an Alpine
15 Watershed, *Water Resour. Res.*, 27(7), 1541–1552, doi:10.1029/91WR00506, 1991.
- 16 Essery, R., Li, L. and Pomeroy, J.: A distributed model of blowing snow over complex
17 terrain, *Hydrol. Process.*, 13(14-15), 2423–2438, doi:10.1002/(SICI)1099-
18 1085(199910)13:14/15<2423::AID-HYP853>3.0.CO;2-U, 1999.
- 19 Farinotti, D., Huss, M., Bauder, A. and Funk, M.: An estimate of the glacier ice volume in the
20 Swiss Alps, *Glob. Planet. Change*, 68(3), 225–231, doi:10.1016/j.gloplacha.2009.05.004,
21 2009.
- 22 Farinotti, D., Magnusson, J., Huss, M. and Bauder, A.: Snow accumulation distribution
23 inferred from time-lapse photography and simple modelling, *Hydrol. Process.*, 24(15), 2087–
24 2097, doi:10.1002/hyp.7629, 2010.
- 25 Frey, S.: Possible Impacts of Climate Change on the Water Balance with Special Emphasis on
26 Runoff and Hydropower Potential, University of Natural Resources and Life Sciences,
27 Vienna. PhD thesis. [online] Available from: <http://permalink.obvsg.at/AC10777542>, 2015.
- 28 Frey, S., Goler, R., Leidinger, D., Formayer, H. and Holzmann, H.: POWERCLIM - Final
29 Report (in German), Vienna., 2014.
- 30 Frey, S. and Holzmann, H.: Berücksichtigung von Schneeverlagerungsprozessen bei der
31 hydrologischen Modellierung alpiner Einzugsgebiete (in German)., in *Tri-Nationaler*
32 *Workshop – Hydrologische Prozesse im Hochgebirge*, Obergurgl, Austria., 2014.
- 33 Fuchs, M.: Auswirkungen von möglichen Klimaänderungen auf die Hydrologie verschiedener
34 Regionen in Österreich. (PhD thesis; in German)., University of Natural Resources and Life
35 Sciences, Vienna., 2005.
- 36 Garvelmann, J., Pohl, S. and Weiler, M.: From observation to the quantification of snow

1 processes with a time-lapse camera network, *Hydrol. Earth Syst. Sci.*, 17(4), 1415–1429,
2 doi:10.5194/hess-17-1415-2013, 2013.

3 Gharari, S., Hrachowitz, M., Fenicia, F., Gao, H. and Savenije, H. H. G.: Using expert
4 knowledge to increase realism in environmental system models can dramatically reduce the
5 need for calibration, *Hydrol. Earth Syst. Sci.*, 18(12), 4839–4859, doi:10.5194/hess-18-4839-
6 2014, 2014.

7 Gharari, S., Hrachowitz, M., Fenicia, F. and Savenije, H. H. G.: Moving beyond traditional
8 model calibration or how to better identify realistic model parameters: sub-period calibration,
9 *Hydrol. Earth Syst. Sci. Discuss.*, 9(2), 1885–1918, doi:10.5194/hessd-9-1885-2012, 2012.

10 Grünewald, T., Bühler, Y. and Lehning, M.: Elevation dependency of mountain snow depth,
11 *Cryosph.*, 8(2013), 2381–2394, doi:10.5194/tc-8-2381-2014, 2014.

12 Gupta, H. V., Kling, H., Yilmaz, K. K. and Martinez, G. F.: Decomposition of the mean
13 squared error and NSE performance criteria: Implications for improving hydrological
14 modelling, *J. Hydrol.*, 377(1-2), 80–91, doi:10.1016/j.jhydrol.2009.08.003, 2009.

15 Gupta, H. V., Wagener, T. and Liu, Y.: Reconciling theory with observations: elements of a
16 diagnostic approach to model evaluation, *Hydrol. Process.*, 22(18), 3802–3813,
17 doi:10.1002/hyp.6989, 2008.

18 Haiden, T., Kann, A., Wittmann, C., Pistotnik, G., Bica, B. and Gruber, C.: The Integrated
19 Nowcasting through Comprehensive Analysis (INCA) System and Its Validation over the
20 Eastern Alpine Region, *Weather Forecast.*, 26(2), 166–183,
21 doi:10.1175/2010WAF2222451.1, 2011.

22 Hall, D. K., Riggs, G. A., Salomonson, V. V., DiGirolamo, N. E. and Bayr, K. J.: MODIS
23 snow-cover products, *Remote Sens. Environ.*, 83(1-2), 181–194, doi:10.1016/S0034-
24 4257(02)00095-0, 2002.

25 Helfricht, K., Schöber, J., Schneider, K., Sailer, R. and Kuhn, M.: Interannual persistence of
26 the seasonal snow cover in a glacierized catchment, *J. Glaciol.*, 60(223), 889–904,
27 doi:10.3189/2014JoG13J197, 2014.

28 Helfricht, K., Schöber, J., Seiser, B., Fischer, A., Stötter, J. and Kuhn, M.: Snow
29 accumulation of a high alpine catchment derived from LiDAR measurements, *Adv. Geosci.*,
30 32, 31–39, doi:10.5194/adgeo-32-31-2012, 2012.

31 Henriksen, H. J., Troldborg, L., Nyegaard, P., Sonnenborg, T. O., Refsgaard, J. C. and
32 Madsen, B.: Methodology for construction, calibration and validation of a national
33 hydrological model for Denmark, *J. Hydrol.*, 280(1-4), 52–71, doi:10.1016/S0022-
34 1694(03)00186-0, 2003.

35 Herrnegger, M., Nachtnebel, H.-P. and Haiden, T.: Evapotranspiration in high alpine
36 catchments – an important part of the water balance!, *Hydrol. Res.*, 43(4), 460,

1 doi:10.2166/nh.2012.132, 2012.

2 Hiebl, J. and Frei, C.: Daily temperature grids for Austria since 1961—concept, creation and
3 applicability, *Theor. Appl. Climatol.*, doi:10.1007/s00704-015-1411-4, 2015.

4 Hiemstra, C. A., Liston, G. E. and Reiners, W. A.: Observing, modelling, and validating snow
5 redistribution by wind in a Wyoming upper treeline landscape, *Ecol. Modell.*, 197(1-2), 35–
6 51, doi:10.1016/j.ecolmodel.2006.03.005, 2006.

7 Hock, R.: Temperature index melt modelling in mountain areas, *J. Hydrol.*, 282(1-4), 104–
8 115, doi:10.1016/S0022-1694(03)00257-9, 2003.

9 Holzmann, H., Lehmann, T., Formayer, H. and Haas, P.: Auswirkungen möglicher
10 Klimaänderungen auf Hochwasser und Wasserhaushaltskomponenten ausgewählter
11 Einzugsgebiete in Österreich (in german), *Österreichische Wasser- und Abfallwirtschaft*,
12 62(1-2), 7–14, doi:10.1007/s00506-009-0154-9, 2010.

13 Hrachowitz, M., Fovet, O., Ruiz, L., Euser, T., Gharari, S., Nijzink, R., Freer, J., Savenije, H.
14 H. G. and Gascuel-Oudou, C.: Process consistency in models: The importance of system
15 signatures, expert knowledge, and process complexity, *Water Resour. Res.*, 50(9), 7445–
16 7469, doi:10.1002/2014WR015484, 2014.

17 Huss, M., Bauder, A. and Funk, M.: Homogenization of long-term mass-balance time series,
18 *Ann. Glaciol.*, 50(50), 198–206, doi:10.3189/172756409787769627, 2009a.

19 Huss, M., Farinotti, D., Bauder, A. and Funk, M.: Modelling runoff from highly glacierized
20 drainage basins in a changing climate, *Mitteilungen der Versuchsanstalt für Wasserbau,
21 Hydrol. und Glaziologie an der Eidgenoss. Tech. Hochschule Zurich*, 22(213), 123–146,
22 doi:10.1002/hyp.7055, 2009b.

23 Jackson, T. H. R.: A Spatially Distributed Snowmelt-Driven Hydrologic Model applied to the
24 Upper Sheep Creek Watershed. PhD thesis., Utah State University, Logan, Utah, USA., 1994.

25 Jonas, T., Marty, C. and Magnusson, J.: Estimating the snow water equivalent from snow
26 depth measurements in the Swiss Alps, *J. Hydrol.*, 378(1-2), 161–167,
27 doi:10.1016/j.jhydrol.2009.09.021, 2009.

28 Kirchner, P. B., Bales, R. C., Molotch, N. P., Flanagan, J. and Guo, Q.: LiDAR measurement
29 of seasonal snow accumulation along an elevation gradient in the southern Sierra Nevada,
30 California, *Hydrol. Earth Syst. Sci. Discuss.*, 11, 5327–5365, doi:10.5194/hessd-11-5327-
31 2014, 2014.

32 Kling, H.: Spatio-Temporal Modelling of the Water Balance of Austria (PhD-thesis),
33 University of Natural Resources and Life Sciences, Vienna., 2006.

34 Kling, H., Fuchs, M. and Paulin, M.: Runoff conditions in the upper Danube basin under an
35 ensemble of climate change scenarios, *J. Hydrol.*, 424-425(0), 264–277,
36 doi:10.1016/j.jhydrol.2012.01.011, 2012.

- 1 Kling, H., Fürst, J. and Nachtnebel, H. P.: Seasonal, spatially distributed modelling of
2 accumulation and melting of snow for computing runoff in a long-term, large-basin water
3 balance model, *Hydrol. Process.*, 20(10), 2141–2156, doi:10.1002/hyp.6203, 2006.
- 4 Kling, H., Stanzel, P., Fuchs, M. and Nachtnebel, H.-P.: Performance of the COSERO
5 precipitation-runoff model under non-stationary conditions in basins with different climates,
6 *Hydrol. Sci. J.*, 141217125340005, doi:10.1080/02626667.2014.959956, 2014a.
- 7 Kling, H., Stanzel, P. and Preishuber, M.: Impact modelling of water resources development
8 and climate scenarios on Zambezi River discharge, *J. Hydrol. Reg. Stud.*, 1, 17–43,
9 doi:10.1016/j.ejrh.2014.05.002, 2014b.
- 10 Koboltschnig, G. R., Schöner, W., Zappa, M., Kroisleitner, C. and Holzmann, H.: Runoff
11 modelling of the glacierized Alpine Upper Salzach basin (Austria): multi-criteria result
12 validation, in *Hydrological Processes*, vol. 22, pp. 3950–3964, John Wiley & Sons, Ltd.,
13 2008.
- 14 Lehning, M., Bartelt, P., Brown, B., Fierz, C. and Satyawali, P.: A physical SNOWPACK
15 model for the Swiss avalanche warning: part II. Snow microstructure, *Cold Reg. Sci.
16 Technol.*, 35(3), 147–167, doi:10.1016/S0165-232X(02)00073-3, 2002.
- 17 Lehning, M. and Fierz, C.: Assessment of snow transport in avalanche terrain, *Cold Reg. Sci.
18 Technol.*, 51(2-3), 240–252, doi:10.1016/j.coldregions.2007.05.012, 2008.
- 19 Liston, G. E.: Representing Subgrid Snow Cover Heterogeneities in Regional and Global
20 Models, *J. Clim.*, 17(6), 1381–1397, doi:10.1175/1520-
21 0442(2004)017<1381:RSSCHI>2.0.CO;2, 2004.
- 22 Liston, G. E., Haehnel, R. B., Sturm, M., Hiemstra, C. a., Berezovskaya, S. and Tabler, R. D.:
23 Simulating complex snow distributions in windy environments using SnowTran-3D, *J.
24 Glaciol.*, 53(181), 241–256, doi:10.3189/172756507782202865, 2007.
- 25 Liston, G. and Sturm, M.: A snow-transport model for complex terrain, *J. Glaciol.*, 44(148),
26 1998.
- 27 Masson, V., Champeaux, J.-L., Chauvin, F., Meriguet, C. and Lacaze, R.: A Global Database
28 of Land Surface Parameters at 1-km Resolution in Meteorological and Climate Models, *J.
29 Clim.*, 16(9), 1261–1282, doi:10.1175/1520-0442-16.9.1261, 2003.
- 30 Mauser, W. and Bach, H.: PROMET - Large scale distributed hydrological modelling to study
31 the impact of climate change on the water flows of mountain watersheds, *J. Hydrol.*, 376(3-4),
32 362–377, doi:10.1016/j.jhydrol.2009.07.046, 2009.
- 33 Melvold, K. and Skaugen, T.: Multiscale spatial variability of lidar-derived and modeled
34 snow depth on Hardangervidda, Norway, *Ann. Glaciol.*, 54(62), 273–281,
35 doi:10.3189/2013AoG62A161, 2013.
- 36 Moore, R. J.: The PDM rainfall-runoff model, *Hydrol. Earth Syst. Sci.*, 11(1), 483–499,

- 1 doi:10.5194/hess-11-483-2007, 2007.
- 2 Nachtnebel, H. P., Baumung, S. and Lettl, W.: Abflussprognosemodell für das Einzugsgebiet
3 der Enns und Steyer (in German), Vienna., 1993.
- 4 Nachtnebel, H. P., Senoner, T., Stanzel, P., Kahl, B., Hernegger, M., Haberl, U. and
5 Pfaffenwimmer, T.: Inflow prediction system for the Hydropower Plant Gabčíkovo, Part 3 -
6 Hydrologic Modelling, Bratislava., 2009.
- 7 Nikulin, G., Kjellström, E., Hansson, U., Strandberg, G. and Ullerstig, A.: Evaluation and
8 future projections of temperature, precipitation and wind extremes over Europe in an
9 ensemble of regional climate simulations, *Tellus A*, 63(1), 41–55, doi:10.1111/j.1600-
10 0870.2010.00466.x, 2011.
- 11 Oubeidillah, A. A., Kao, S.-C., Ashfaq, M., Naz, B. S. and Tootle, G.: A large-scale, high-
12 resolution hydrological model parameter data set for climate change impact assessment for
13 the conterminous US, *Hydrol. Earth Syst. Sci.*, 18(1), 67–84, doi:10.5194/hess-18-67-2014,
14 2014.
- 15 Pohl, S., Garvelmann, J., Wawerla, J. and Weiler, M.: Potential of a low-cost sensor network
16 to understand the spatial and temporal dynamics of a mountain snow cover, *Water Resour.*
17 *Res.*, 50(3), 2533–2550, doi:10.1002/2013WR014594, 2014.
- 18 Pomeroy, J. W., Gray, D. M., Hedstrom, N. R. and Janowicz, J. R.: Prediction of seasonal
19 snow accumulation in cold climate forests, *Hydrol. Process.*, 16(18), 3543–3558,
20 doi:10.1002/hyp.1228, 2002.
- 21 Pomeroy, J. W., Gray, D. M., Shook, K. R., Toth, B., Essery, R. L. H., Pietroniro, A. and
22 Hedstrom, N.: An evaluation of snow accumulation and ablation processes for land surface
23 modelling, *Hydrol. Process.*, 12(15), 2339–2367, doi:10.1002/(SICI)1099-
24 1085(199812)12:15<2339::AID-HYP800>3.0.CO;2-L, 1998.
- 25 Prasad, R., Tarboton, D. G., Liston, G. E., Luce, C. H. and Seyfried, M. S.: Testing a blowing
26 snow model against distributed snow measurements at Upper Sheep Creek, Idaho, United
27 States of America, *Water Resour. Res.*, 37(5), 1341–1356, doi:10.1029/2000WR900317,
28 2001.
- 29 Rasmussen, R. M., Hallett, J., Purcell, R., Landolt, S. D. and Cole, J.: The hotplate
30 precipitation gauge, *J. Atmos. Ocean. Technol.*, 28, 148–164,
31 doi:10.1175/2010JTECHA1375.1, 2011.
- 32 Riley, J., Israelsen, E. and Eggleston, K.: Some approaches to snowmelt prediction, *Role*
33 *Snowmelt Ice Hydrol. IAHS Publ.* 107, 956–971, 1973.
- 34 Rosenbrock, H.: An automatic method for finding the greatest or least value of a function,
35 *Comput. J.*, 3(3), 175–184, doi:10.1093/comjnl/3.3.175, 1960.
- 36 Rutter, N., Essery, R., Pomeroy, J., Altimir, N., Andreadis, K., Baker, I., Barr, A., Bartlett, P.,

- 1 Boone, A., Deng, H., Douville, H., Dutra, E., Elder, K., Ellis, C., Feng, X., Gelfan, A.,
2 Goodbody, A., Gusev, Y., Gustafsson, D., Hellström, R., Hirabayashi, Y., Hirota, T., Jonas,
3 T., Koren, V., Kuragina, A., Lettenmaier, D., Li, W. P., Luce, C., Martin, E., Nasonova, O.,
4 Pumpanen, J., Pyles, R. D., Samuelsson, P., Sandells, M., Schädler, G., Shmakin, A.,
5 Smirnova, T. G., Stähli, M., Stöckli, R., Strasser, U., Su, H., Suzuki, K., Takata, K., Tanaka,
6 K., Thompson, E., Vesala, T., Viterbo, P., Wiltshire, A., Xia, K., Xue, Y. and Yamazaki, T.:
7 Evaluation of forest snow processes models (SnowMIP2), *J. Geophys. Res. Atmos.*, 114,
8 doi:10.1029/2008JD011063, 2009.
- 9 Safeeq, M., Mauger, G. S., Grant, G. E., Arismendi, I., Hamlet, A. F. and Lee, S.-Y.:
10 Comparing Large-Scale Hydrological Model Predictions with Observed Streamflow in the
11 Pacific Northwest: Effects of Climate and Groundwater*, *J. Hydrometeorol.*, 15(6), 2501–
12 2521, doi:10.1175/JHM-D-13-0198.1, 2014.
- 13 Schaefli, B., Hingray, B., Niggli, M. and Musy, A.: A conceptual glacio-hydrological model
14 for high mountainous catchments, *Hydrol. Earth Syst. Sci.*, 9(1/2), 95–109, doi:10.5194/hess-
15 9-95-2005, 2005.
- 16 Schöber, J., Schneider, K., Helfricht, K., Schattan, P., Achleitner, S., Schöberl, F. and
17 Kirnbauer, R.: Snow cover characteristics in a glacierized catchment in the Tyrolean Alps -
18 Improved spatially distributed modelling by usage of Lidar data, *J. Hydrol.*, 519, 3492–3510,
19 doi:10.1016/j.jhydrol.2013.12.054, 2014.
- 20 Scipión, D. E., Mott, R., Lehning, M., Schneebeli, M. and Berne, A.: Seasonal small-scale
21 spatial variability in alpine snowfall and snow accumulation, *Water Resour. Res.*, 49, 1446–
22 1457, doi:10.1002/wrcr.20135, 2013.
- 23 Shulski, M. D. and Seeley, M. W.: Application of Snowfall and Wind Statistics to Snow
24 Transport Modeling for Snowdrift Control in Minnesota, *J. Appl. Meteorol.*, 43(11), 1711–
25 1721, doi:10.1175/JAM2140.1, 2004.
- 26 Sovilla, B., Mcelwaine, J. N., Schaer, M. and Vallet, J.: Variation of deposition depth with
27 slope angle in snow avalanches: Measurements from Vallée de la Sionne., 2010.
- 28 Stanzel, P., Kahl, B., Haberl, U., Herrnegger, M. and Nachtnebel, H. P.: Continuous
29 hydrological modelling in the context of real time flood forecasting in alpine Danube tributary
30 catchments, *IOP Conf. Ser. Earth Environ. Sci.*, 4, 012005, doi:10.1088/1755-
31 1307/4/1/012005, 2008.
- 32 Stanzel, P. and Nachtnebel, H. P.: Mögliche Auswirkungen des Klimawandels auf den
33 Wasserhaushalt und die Wasserkraftnutzung in Österreich (in German), *Österreichische*
34 *Wasser- und Abfallwirtschaft*, 62(9-10), 180–187, doi:10.1007/s00506-010-0234-x, 2010.
- 35 Strasser, U., Bernhardt, M., Weber, M., Liston, G. E. and Mauser, W.: Is snow sublimation
36 important in the alpine water balance?, *Cryosph.*, 2, 53–66, doi:10.5194/tc-2-53-2008, 2008.
- 37 Thornthwaite, C. W.: An Approach toward a Rational Classification of Climate, *Geogr. Rev.*,

- 1 38(1), 55–94, 1948.
- 2 Weber, M., Braun, L., Mauser, W. and Prasad, W.: Contribution of rain, snow- and icemelt in
3 the upper Danube discharge today and in the future, *Geogr. Fis. e Din. Quat.*, 33(2), 221–230,
4 2010.
- 5 Williams, M. W., Bardsley, T. and Ridders, M.: Overestimation of snow depth and inorganic
6 nitrogen wetfall using NADP data, Niwot Ridge, Colorado, *Atmos. Environ.*, 32, 3827–3833,
7 doi:10.1016/S1352-2310(98)00009-0, 1998.
- 8 Winstral, A., Elder, K. and Davis, R. E.: Spatial Snow Modeling of Wind-Redistributed Snow
9 Using Terrain-Based Parameters, *J. Hydrometeorol.*, 3(5), 524–538, doi:10.1175/1525-
10 7541(2002)003<0524:SSMOWR>2.0.CO;2, 2002.
- 11 Wood, E. F., Lettenmaier, D. P. and Zartarian, V. G.: A land-surface hydrology
12 parameterization with subgrid variability for general circulation models, *J. Geophys. Res.*,
13 97(D3), 2717, doi:10.1029/91JD01786, 1992.
- 14

1 Table 1. Land use classes used in COSERO (derived from CORINE land cover data, EEA,
 2 1995) and their proportion in the Ötztal. Snow holding capacities H_v for each type of land use
 3 are taken from (Liston and Sturm, 1998; Prasad et al., 2001).

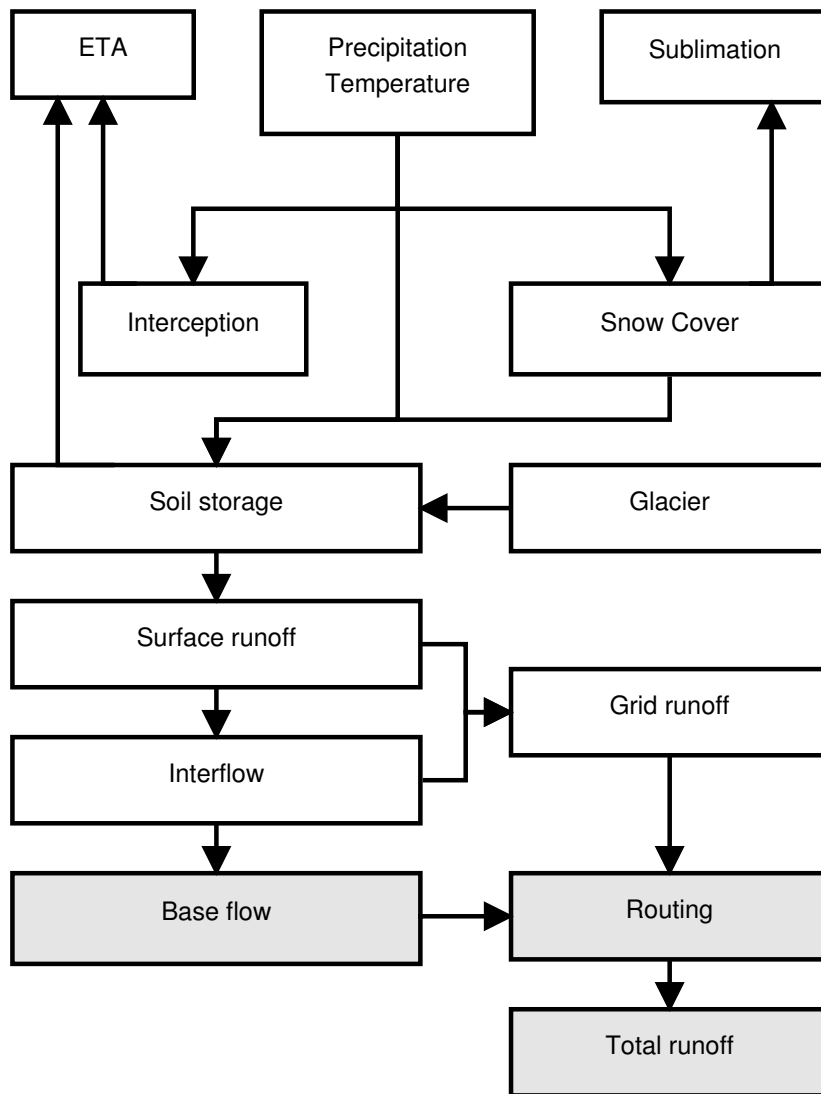
Land use class	proportion [%]	Snow holding capacity H_v [mm]
Build-up areas	1.2	100
Pastures and meadows	20.9	500
Coniferous forests	8.1	2500
Sparsely vegetated areas	20.9	300
Bare rocks	29.5	200
Glaciers	19.4	200

4

1 Table 2. Comparison of performances of model A and B with respect to snow cover and
 2 runoff. For snow cover coefficient of determination (R^2) was used, whereas Kling-Gupta-
 3 Efficiency (Gupta et al., 2009) was used for runoff.

	Calibration		Validation	
	Snow cover	Runoff	Snow cover	Runoff
	(R^2)	(KGE)	(R^2)	(KGE)
MODEL A	0.78	0.93	0.74	0.92
MODEL B	0.70	0.88	0.66	0.90

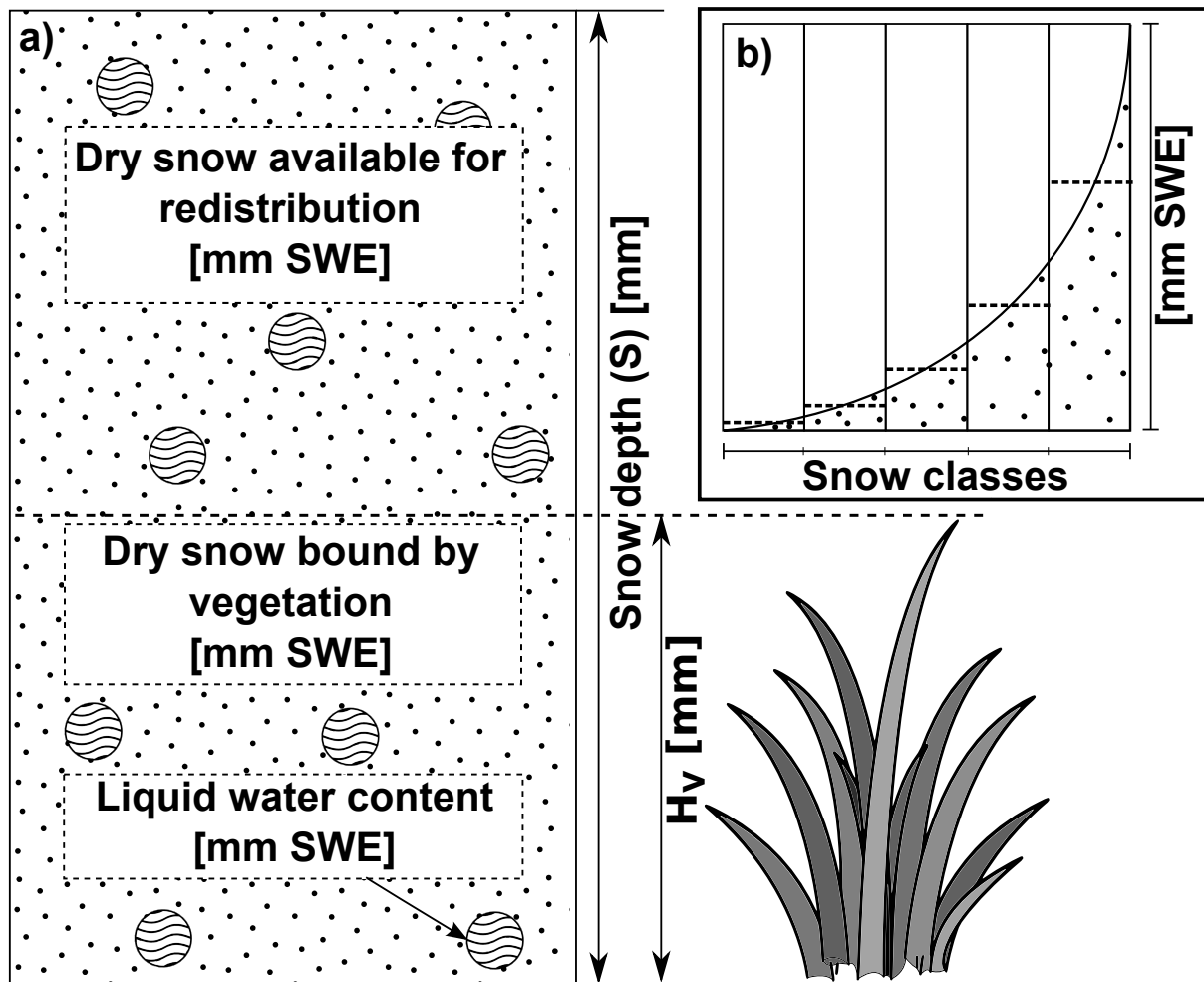
4



1

2

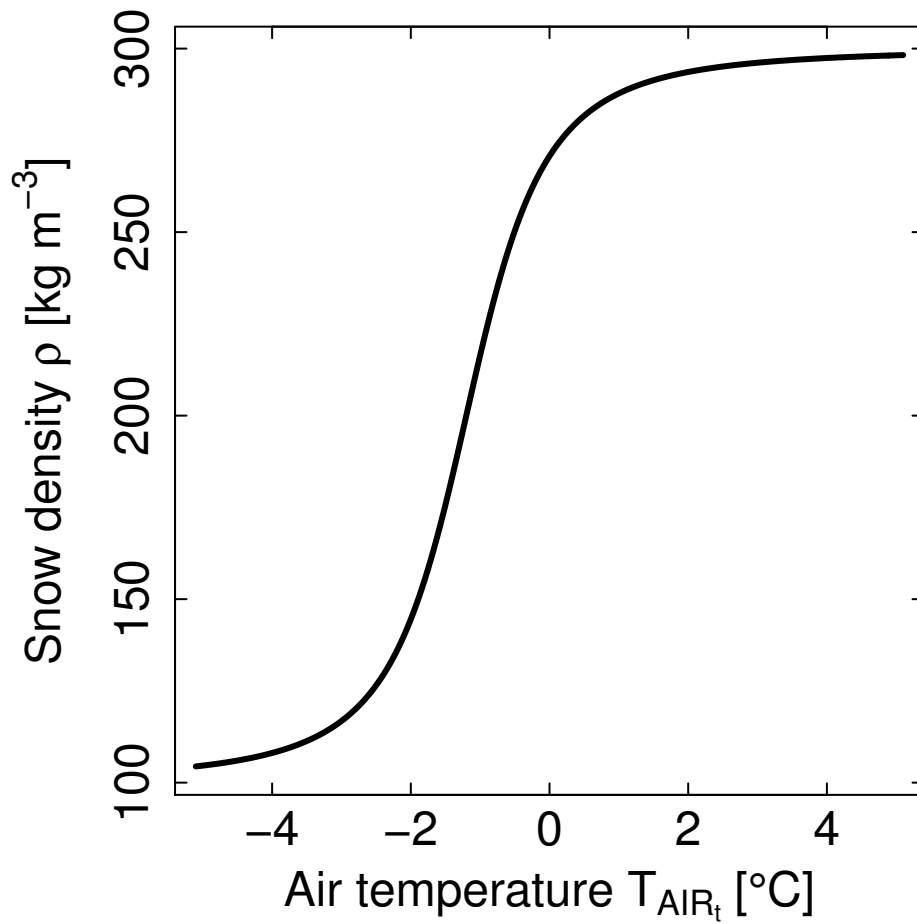
3 Figure 1. Flow chart of the conceptual model COSERO. White parts represent distributed
 4 processes, greyish parts are calculated on a subbasin scale. Snow transport is implemented in
 5 the snow cover module.



1

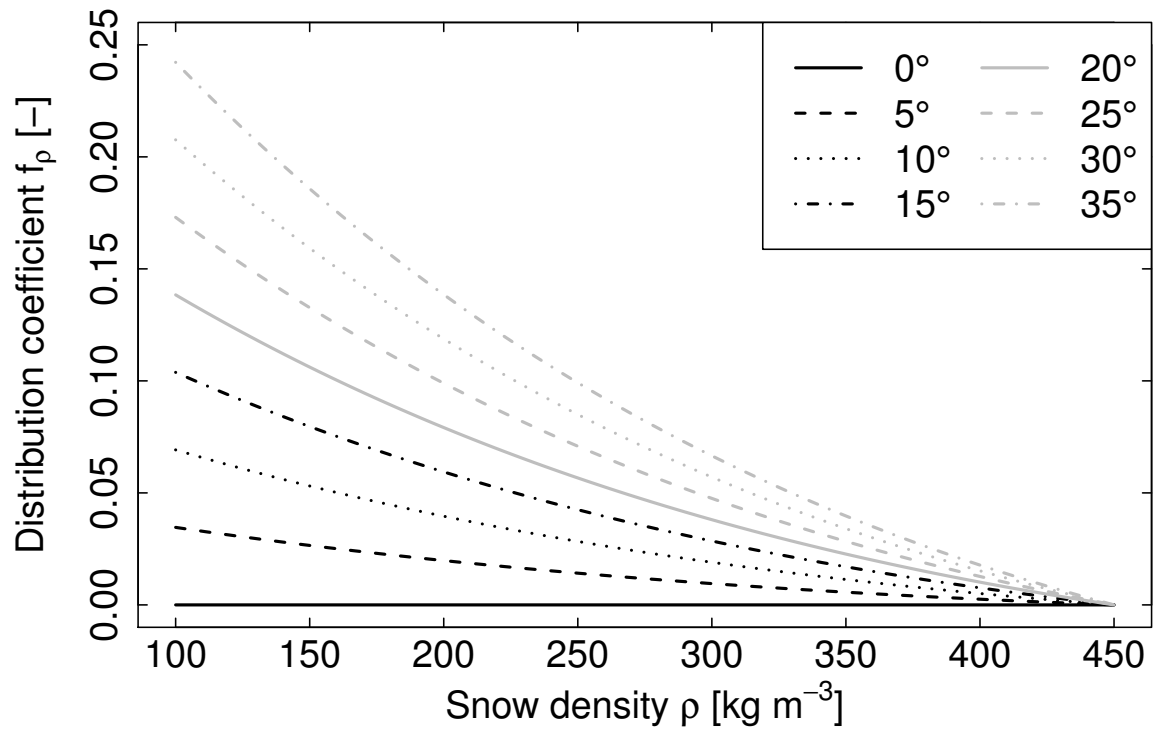
2

3 Figure 2. Schematic view of the snow cover in COSERO. a) Composition of one snow class.
 4 Vegetation or surface roughness defines the threshold value (H_v) to hold back an amount of
 5 snow. b) View of one grid cell including five snow classes each of which is composed in the
 6 way shown in a). Snowfall is distributed log-normally throughout the classes (dashed lines in
 7 b)). Note that snow depth S is given in mm while all other parameters regarding snow are
 8 given in mm SWE.



1
2
3
4
5

Figure 3. Estimation of the density of snow using Eqs. (8) and (9). Minimum and maximum densities of fresh snow are 100 and 300 kg m⁻³, respectively.

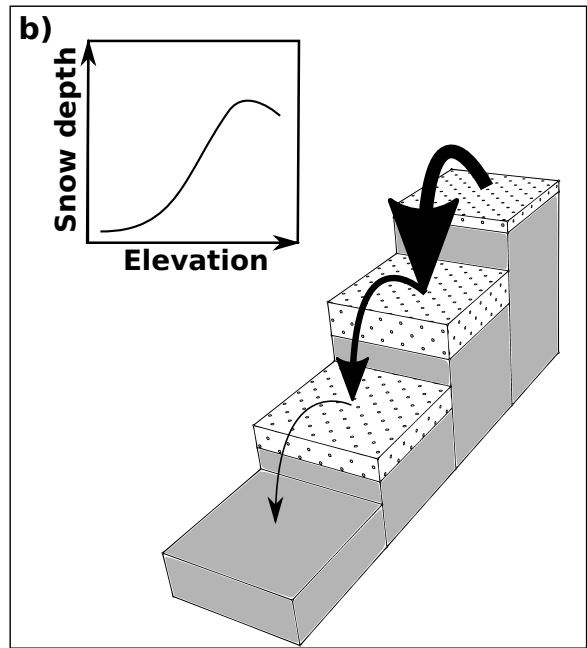
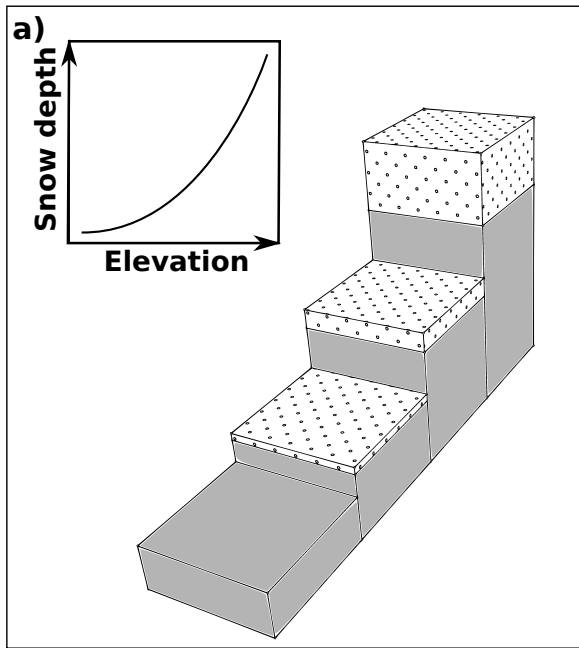


1

2

3 Figure 4. Shapes of the distribution coefficient in dependency of different slope angles and

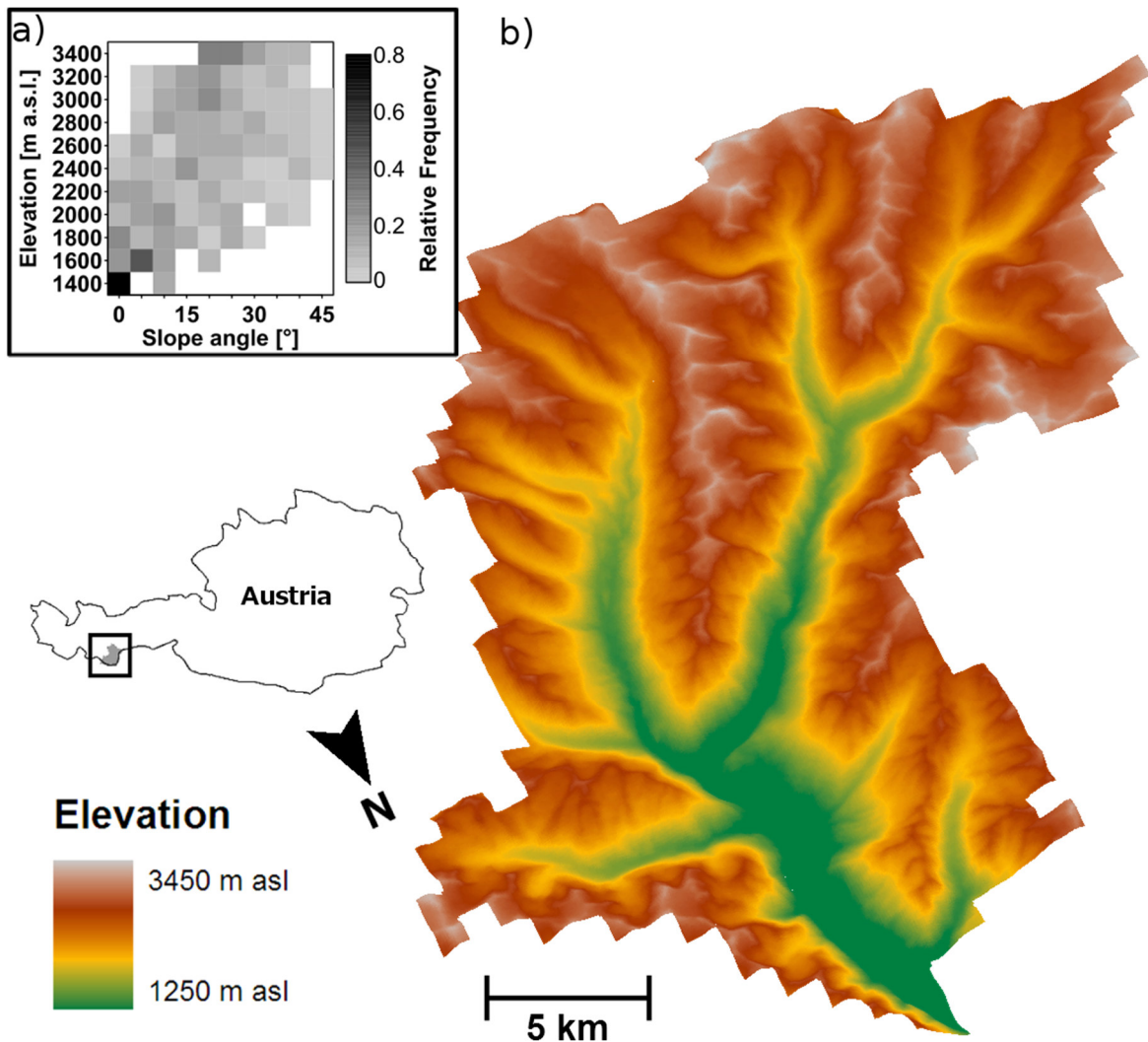
4 snow densities.



1

2

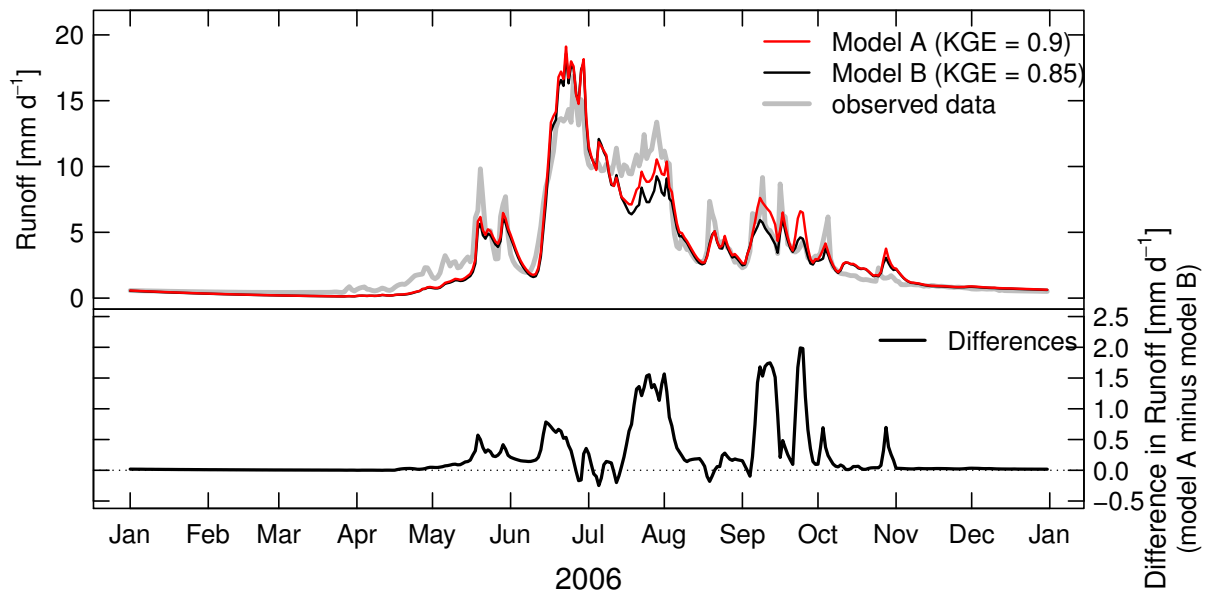
3 Figure 5. Conceptual snow accumulations in mountainous regions without (a) and with (b)
 4 considering lateral snow transport processes. Dotted blocks represent exaggerated snow
 5 accumulations.



1

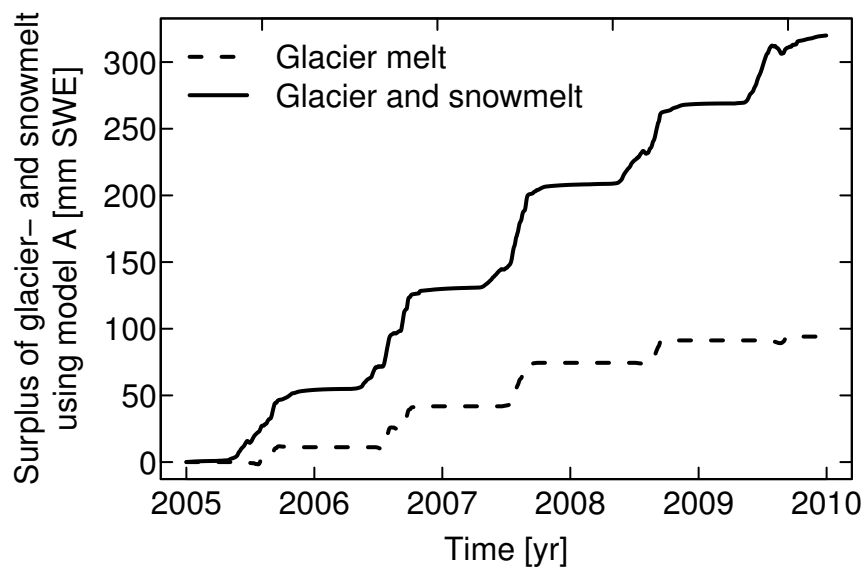
2

3 Figure 6. Elevation levels of the Ötztal using a 1x1 km grid (b). Frequency distribution of
 4 slope angles derived from 1x1 km grid are shown (a). Slopes in general are steeper in the
 5 summit regions than in the valleys. Note that instead of the average slope of a grid cell only
 6 steepest vertical gradients are plotted.



1
2

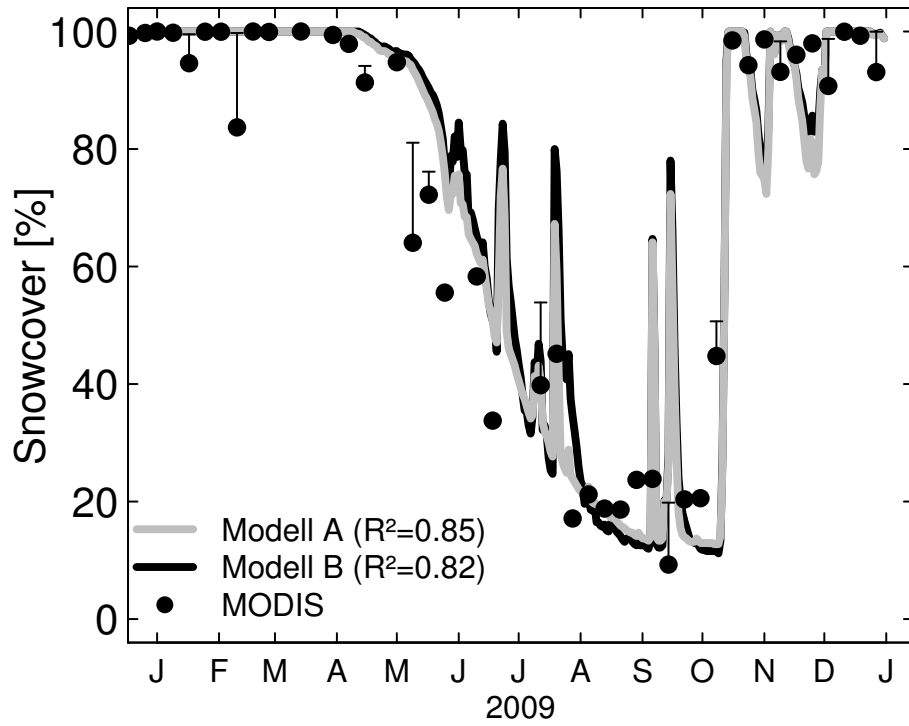
3 Figure 7. Specific runoff at the outlet at Huben is modelled with (model A) and without
4 (model B) using the snow redistribution routine.



1

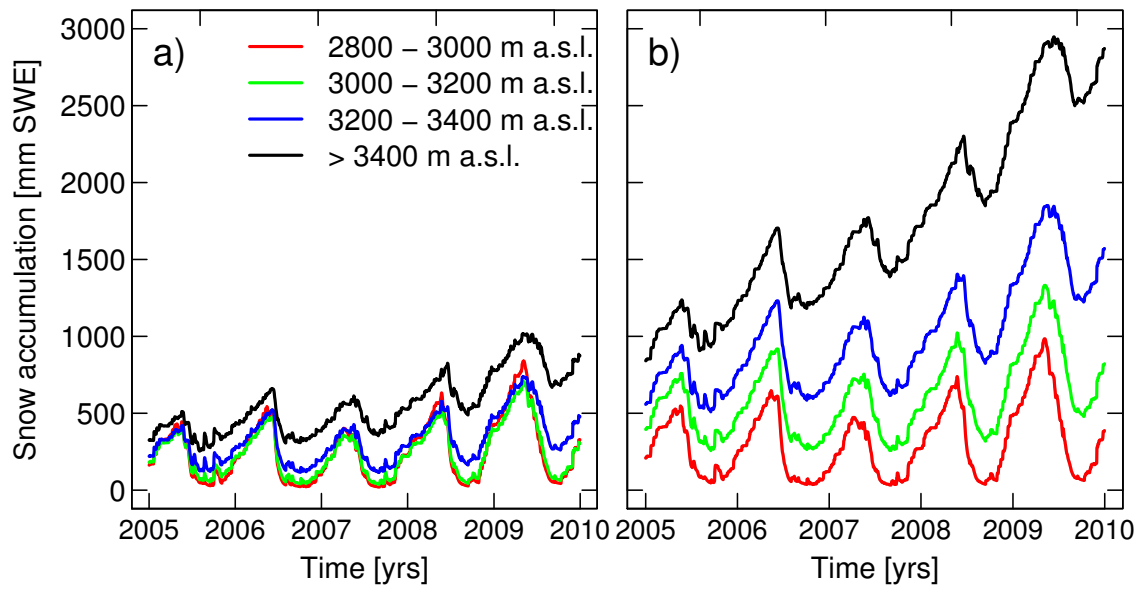
2

3 Figure 8. Accumulated differences (model A minus model B) in discharge at gauge Huben.



1
2
3
4
5

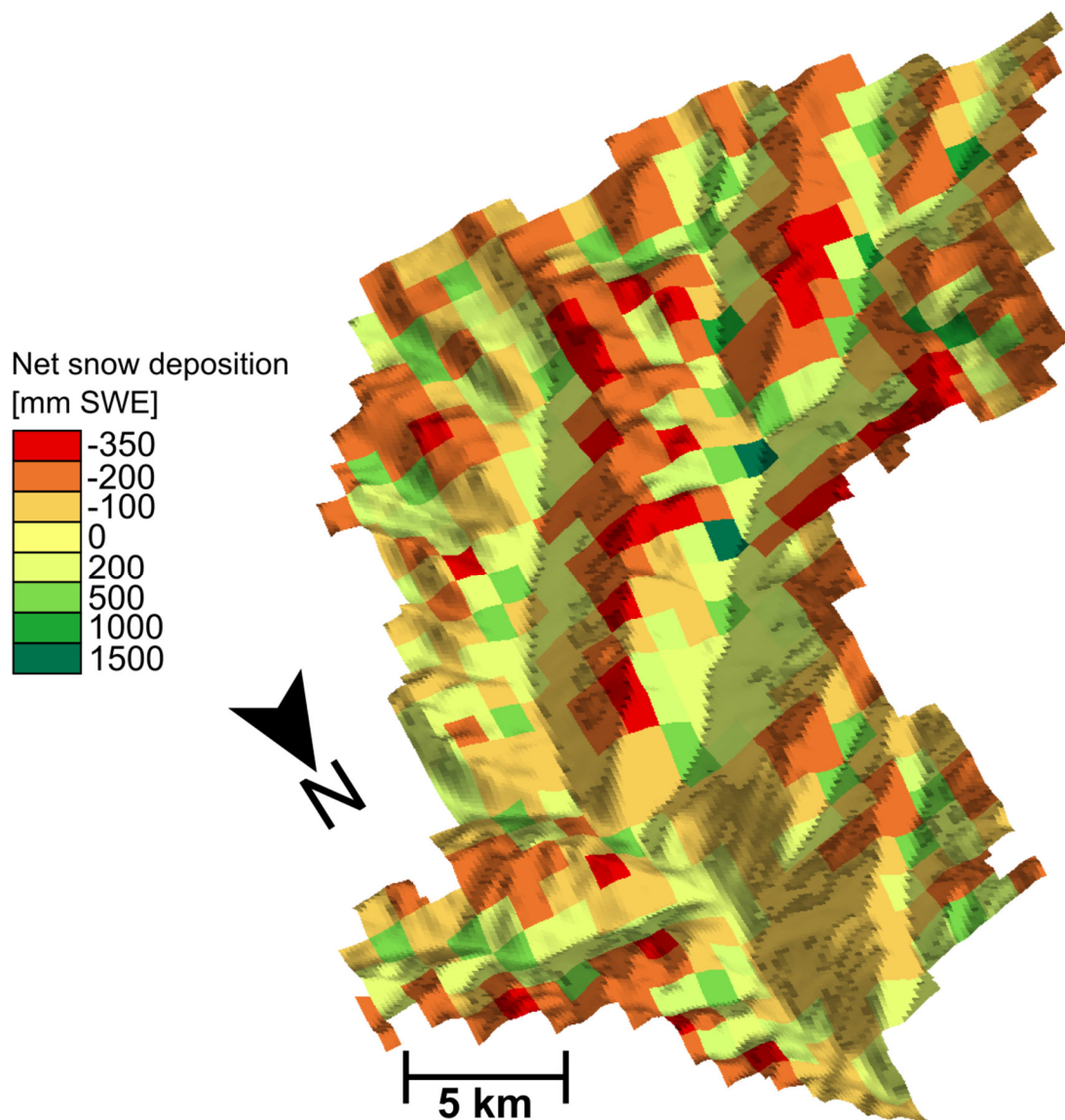
Figure 9. Snow cover in 2009 modelled by both model A and B compared with MODIS data. Error bars refer to uncertainties due to cloud coverage.



1

2

3 Figure 10. Behaviour of snow accumulation and melt of model A (a) and B (b) in the upper
 4 elevations. Note that model results are shown from 2005 to 2010 without the warm-up period
 5 for clarity reasons. Therefore snow depth does not start at zero in the figure while it does at
 6 the beginning of the modelling.



1

2

3 Figure 11. Net snow deposition in the catchment during the time period of one year. Negative
 4 values refer to a net loss, positive to a net gain of snow. Note that, since only the net
 5 deposition of snow based on lateral transport is shown, values cannot be linked to snow
 6 depths at the end of the time period.